Available online at www.sciencedirect.com
ScienceDirect
JOURNAL OF IRON AND STEEL RESEARCH, INTERNATIONAL. 2016, 23(3): 220-224

One-step Crystallization Kinetic Parameters of the Glass-ceramics Prepared from Stainless Steel Slag and Pickling Sludge

Shen-gen ZHANG[1], Jian YANG[1], Bo LIU[1], De-an PAN[1], Chun-li WU[1], Alex A. VOLINSKY[2]

(1. Institute for Advanced Materials and Technology, School of Materials Science and Engineering, University of Science and Technology Beijing, Beijing 100083, China; 2. Department of Mechanical Engineering, University of South Florida, Tampa 33620, Florida, USA)

Abstract: One-step crystallization is one of the most energy conserving methods for glass-ceramics preparation. However, only a few kinetics studies focused on the glass-ceramics prepared by the one-step crystallization. The one-step crystallization kinetic parameters were studied using differential scanning calorimetry. The activation energy (E_a) and the Avrami parameter (n) were calculated as 152.79 kJ·mol^{-1} and 4.39, respectively. These parameters indicate that continuous nucleation and three-dimensional crystal growth are the dominating mechanisms in the one-step crystallization process of the parent glass. The properties of the obtained glass-ceramics can be compared to the glass-ceramics prepared by the two-stage heat treatment and sintering method. This crystallization kinetics research can be used to evaluate the one-step crystallization potential of a parent glass.

Key words: glass-ceramics; one-step crystallization; crystallization kinetics; continuous nucleation

Glass-ceramics are fine-grained polycrystalline materials produced by vitrification and subsequent heat treatment processing[1]. Traditional heat treatment methods for glass-ceramics production are sintering and two-stage heat treatment, which are energy intensive and expensive[2,3]. Therefore, it is necessary to develop a more economical heat treatment route for glass-ceramics production[4,5]. The best candidate may be the one-step heat treatment process, since both nucleation and crystallization take place in the same heating process during the one-step heat treatment[6]. Thus, the advantages of the one-step heat treatment are shorter process flow and lower production cost, in line with the requirements for energy-savings and emissions reduction.

The blast furnace slag glass-ceramics was successfully prepared for the first time using the one-step heat treatment with proper nucleation agent[7]. The obtained glass-ceramics system is known as "sliceram". The "sliceram" has attracted attention from a lot of researchers. However, as far as known, there were few crystallization kinetics studies focused on the one-step crystallization of glass-ceramics. And the crystallization kinetics characteristic parameters of the parent glass were unclear. Thus, no dynamic indexes, such as crystallization activation energy and Avrami parameter, can be used to evaluate the one-step crystallization potential of a parent glass so far. Therefore, it is significant to research the crystallization kinetics issues of the glass-ceramics prepared by one-step crystallization.

This research focused on the one-step crystallization kinetics of the glass-ceramics preparation. The kinetic parameters and crystallization mechanism of the glass, which can be prepared by the one-step crystallization, were studied. The crystallization activation energy, the Avrami parameter and the microstructure were evaluated.

Foundation Item: Item Sponsored by National Natural Science Foundation of China (U1360202, 51472030, 51502014); National Key Project of the Scientific and Technical Support Program of China (2011BAE13B07, 2012BAC02B01, 2011BAC10B02); National Hi-tech Research and Development Program of China (2012AA063202); Fundamental Research Funds for the Central Universities of China (FRF-TP-15-050A2); China Postdoctoral Science Foundation Funded Project (2014M560885)

Biography: Shen-gen ZHANG, Doctor, Professor; **E-mail**: zhangshengen@mater.ustb.edu.cn; **Received Date**: June 17, 2015

Corresponding Author: Bo LIU, Doctor, Assistant Research Fellow; **E-mail**: liubo706@126.com

1 Experimental Procedure

The stainless steel slag was obtained from Qingshan Jinhui Stainless Steel Industry Co., Ltd. in Henan, China. Baosteel Group Co., Ltd. in Shanghai, China provided the pickling sludge. And the cullet was obtained by grinding down the waste glass from common soda-glass. According to the burdening optimization experiment, the dried fine powders of 37.8 mass% stainless steel slag, 14.0 mass% pickling sludge and 48.2 mass% cullet were mixed together by ball-milling for 1 h. The mixed powder was melted in a muffle furnace at 1460 ℃ for 1 h. Then, the melt was cast into a preheated steel plate and annealed at 600 ℃ for 30 min to release the thermal stresses, followed by slow cooling to room temperature to obtain the parent glass. Table 1 shows the chemical compositions of raw materials and the parent glass. The one-step crystallization route of the glass-ceramics is shown in Fig. 1.

Table 1 Chemical compositions of raw materials and parent glass mass%

Sample	CaO	MgO	SiO_2	Al_2O_3	Fe_2O_3	Na_2O	CaF_2	SO_3	Others
SSS	36.97	26.11	21.46	6.46	2.51	0.08	2.12	1.22	3.07
Cullet	9.04	4.08	68.30	2.49	0.59	14.37	—	0.37	0.76
PS	0	1.17	9.30	2.72	25.52	1.74	45.71	4.38	9.46
Present glass	18.33	12.00	42.34	4.02	4.80	7.20	7.20	1.25	2.86

Note: 1) SSS represents stainless steel slag; 2) PS represents pickling sludge; 3) Others represent TiO_2, Cr_2O_3, NiO, MnO, and CuO, and so on.

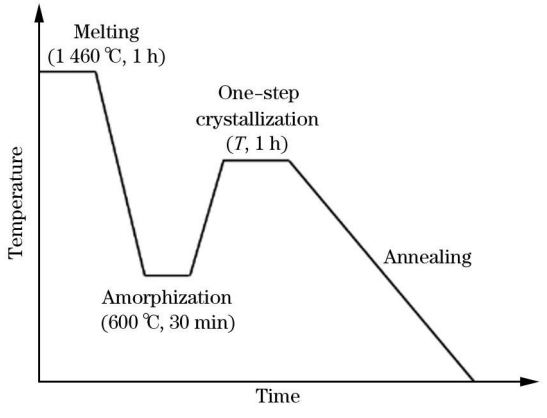

The following one-step crystallization temperatures were used: T = 680 ℃, 705 ℃, 730 ℃, 780 ℃, 830 ℃, 880 ℃ and 930 ℃.

Fig. 1 One-step crystallization preparation methods of glass-ceramics

Differential scanning calorimetry (DSC) measurements were carried out for the powdered glass specimens with NETZSCH STA 409 C/CD analyzer at a heating rate of 10 ℃ · min^{-1}, 20 ℃ · min^{-1}, 30 ℃ · min^{-1} and 40 ℃ · min^{-1} from room temperature to 1000 ℃, to evaluate the glass crystallization activation energy (E_a) and the Avrami parameter (n).

The crystalline phases of the glass-ceramics samples were identified using X-ray diffraction (XRD) with copper target operated at 40 kV and 150 mA, in the 2θ (θ is diffraction angle) range of 10° to 90° and the scan rate of 10(°)/min. Scanning electron microscopy (SEM, Carl Zeiss EVO 18) analysis was carried out on the etched fracture surface of the glass-ceramics.

Vickers hardness was measured using a Vickers hardness testing machine (MH-6 Instrument, Shanghai, China), with load of 2 N and loading time of 10 s. Microcomputer-controlled precision ceramic testing machine, CDW-5 (China), was employed to test the bending strength using the 3-point bending geometry. The bulk density of the samples was tested by the Archimedes method.

2 Results and Discussion

Fig. 2 shows the DSC curves of the parent glass at different heating rates (α) from 10 to 40 ℃ · min^{-1}. It can be seen that there is only one exothermic peak present in the DSC curves. The glass transition temperature (T_g), peak crystallization temperature (T_p), glass working range ($\Delta T = T_p - T_g$) and full width at half maximum of the exothermic peak (ΔT_{FWHM}) of the parent glass are listed in Table 2. T_g and T_p were obtained as 630.8 − 636.5 ℃ and

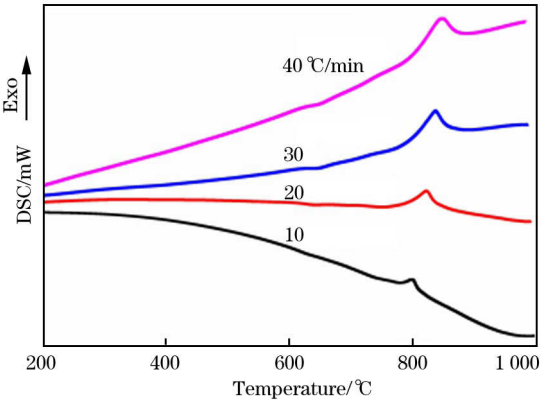

Fig. 2 DSC curves of the glass at different heating rates

Table 2 Parent glass crystallization peak temperatures at different heating rates

α/(℃ · min^{-1})	T_g/℃	T_p/℃	ΔT/℃	ΔT_{FWHM}/℃
10	630.8±1	798.7±1	167.9±1	27.4±1
20	633.6±1	821.0±1	187.4±1	36.9±1
30	634.9±1	834.8±1	199.9±1	41.7±1
40	636.5±1	844.9±1	208.4±1	49.2±1

798.7—844.9 ℃, respectively. As seen in Table 2, increasing the heating rate results in higher T_g and T_p. ΔT was found to be 167.9—208.4 ℃. With higher heating rate, ΔT_{FWHM} increased from 27.4 ℃ to 49.2 ℃. All values of T_g, T_p, ΔT and ΔT_{FWHM} depend on the heating rate.

Regarding the kinetic parameters, E_a and n are the key parameters to judge the crystallization capability of the glass[8]. Thus, the crystallization kinetic parameters of the parent glass were studied by DSC with four different heating rates varying from 10 ℃ · min^{-1} to 40 ℃ · min^{-1}. The E_a of the crystallization was calculated using the Kissinger equation[9]:

$$\ln\left(\frac{\alpha}{T_p^2}\right)=-\frac{E_a}{RT_p}+C \tag{1}$$

where, R is the gas constant, 8.314 J · mol^{-1} · K^{-1}; and C is a constant. Fig. 3 shows the plot of $\ln(\alpha/T_p^2)$ versus $1000/T_p$ for the parent glass. The E_a calculated from the slope of the plot is 152.79 kJ/mol.

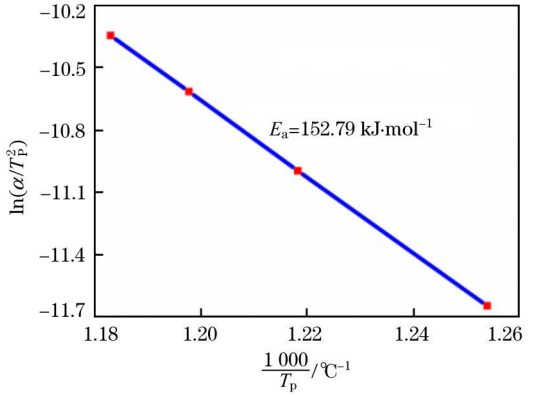

Fig. 3 Plot of $\ln(\alpha/T_p^2)$ versus $1000/T_p$ for the parent glass

In order to determine the crystallization mechanism, the Avrami parameter was calculated using the Augis-Bennett equation[9,10]:

$$n=\frac{2.5}{\Delta T_{FWHM}}\times\frac{RT_p^2}{E_a} \tag{2}$$

The n value of the parent glass was determined as 4.39. The crystallization kinetic parameters of the parent glass and other relative glasses are listed in Table 3.

Table 3 Crystallization kinetic parameters of the present glass and comparison with the literature-reported CaO-MgO-SiO_2-Al_2O_3 glass system

Sample	Present glass	AR[11]	M3[12]	W[13]	FT[10]
E_a/(kJ · mol^{-1})	152.79	253.6	255.75	201.28	338.9
n	4.39	3.23	3.57	—	2

Note: AR, M3, W and FT are the sample names.

Generally, the E_a value is related to the energy barrier when the glass matrix transforms into the crystallized phase. The phase transition will be easier for the glass to crystallize if the E_a is lower[8,10]. As shown in Table 3, the calculated E_a value of the parent glass is lower than those of the other glasses, which means that the obtained glass will crystallize more easily compared with other samples. Besides, the Avrami parameter is related to the crystallization manner: $n=1$ indicates surface crystallization; $n=2$ indicates two-dimensional growth; $n=3$ implies bulk crystallization[10,11]. Malek[12] summarized the meanings of n at the nucleation stage: $3<n<4$ implied decreasing the nucleation rate (site saturation); $n=4$ indicated constant nucleation rate; $n>4$ implied increasing nucleation rate. In Table 3, the n value of the parent glass is greater than 4. Although high n value has been reported[13], it was unexpected in this study. This high n value was caused by both the nucleation frequency and the crystal growth rate, which has the power-law time dependence[14,15]. E_a and n were calculated as 152.79 kJ/mol and 4.39, respectively. This indicates that continuous nucleation and three-dimensional crystal growth are the dominating mechanisms in the crystallization process of the parent glass. Based on these kinetic parameters, it is reasonable to infer that the crystallization rate increases with the crystallized fraction.

The formal theory of transformation kinetics was employed to confirm this. The crystallized volume fraction (χ) is expressed in terms of the crystal growth (μ) as a function of time (t) as follows[16]:

$$\chi=1-\exp\{[-g\int_0^t\mu(t)\mathrm{d}t]^m\} \tag{3}$$

where, g is a geometric factor; and m is an exponent related to the dimensionality of the crystal growth. The kinetics exponent is $n=m$, assuming an Arrhenius temperature dependence of μ. The crystallized fraction was determined from the DSC curves using Eq. (4)[17,18]:

$$\chi(T)=\frac{A_{\Delta T}}{A_{total}} \tag{4}$$

where, $\chi(T)$ is the crystallized fraction at the temperature T; $A_{\Delta T}$ is the area at the temperature interval ΔT; and A_{total} is the total area of the crystallization peak. Fig. 4 shows $\chi(T)$ versus temperature for the crystallization peak of the parent glass at four different heating rates varying from 10 to 40 ℃ · min^{-1}. The S-type χ-T curves indicate that the crystallization process was slow at the beginning stage. Then, the χ rapidly increased in the range of $0.1<\chi<0.8$. These results confirm that the crystallization rate increases with the crystallization fraction at the beginning and the middle stages. Besides, these results also verify that the continuous nucleation is the dominating mechanism of the one-step crystallization process of the parent glass.

Generally, the three-dimensional crystal growth contributes to granular crystals. Thus, to obtain the phase composition and microstructure information of the one-step crystallization, the parent glass was one-step heat treated at 680—930 ℃ for 1 h. The XRD results (Fig. 5 (a)) indicate that the parent glass was an amorphous material. Fig. 5(a) demonstrates that above 730 ℃, numerous crystalline phases were formed in the initial amorphous glass during the one-step heat treatment process: augite ($Ca(Mg,Fe,Al)(Si,Al)_2O_6$, PDF # 24-0202) and cuspidine ($Ca_4Si_2O_7F_2$, PDF # 41-1471). These results indicate that the crystallization process finished during the one-step heat treatment. Besides, the strongest diffraction peak position of the augite shifted to lower 2θ, as seen in Fig. 5 (b). Based on the Bragg's equation ($2d\sin\theta = n_1\lambda$, where d is interplanar spacing, n_1 is diffraction series, and λ is the wavelength of the incident X-ray), the distance between the crystalline faces of augite increased with the heat treatment temperature.

The heat treated glass-ceramics samples were analyzed by SEM. In Fig. 6(a), there are no crystal particles observed in the parent glass, confirming that no crystalline nuclei formed in the annealed glass. As seen in Figs. 6(d)—6(h), the crystallization was almost complete above 730 ℃ via bulk crystallization. Homogeneous granular particles with the size of less than 2 μm can be observed in Figs. 6(d)—6(h), without any coarse crystals. This indicated that the Ostwald ripening process did not occur during the

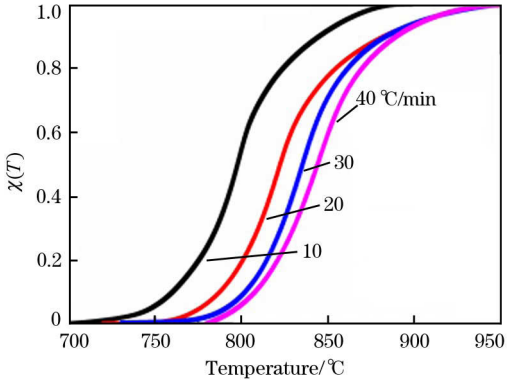

Fig. 4 Crystallized fraction as a function of temperature at different heating rates

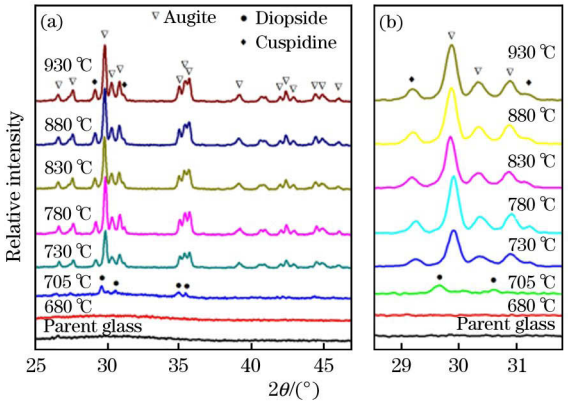

Fig. 5 XRD of the samples after heat treatment at different temperatures for 1 h (a) and detailed XRD patterns (b)

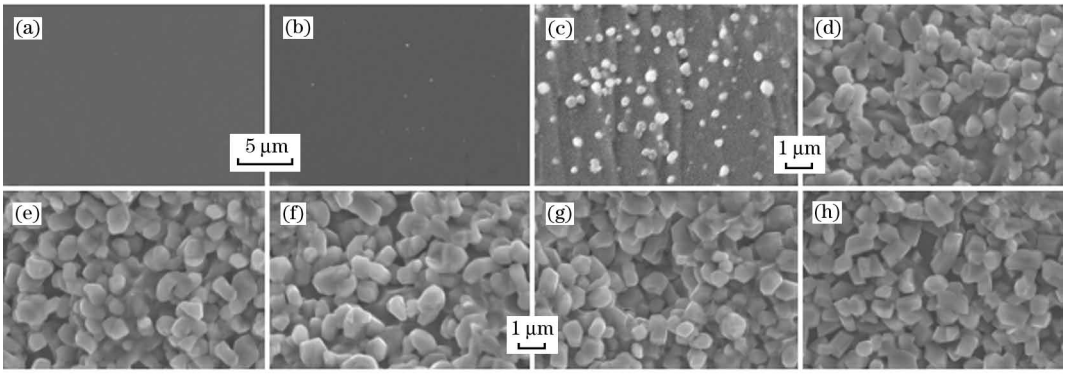

(a) 600 ℃; (b) 680 ℃; (c) 705 ℃; (d) 730 ℃; (e) 780 ℃; (f) 830 ℃; (g) 880 ℃; (h) 930 ℃.

Fig. 6 SEM images of the glass-ceramics heat treated at different temperatures for 1 h

heat treatment, even though the heat treatment temperature was higher than the exothermal peak temperature in Fig. 2. The XRD and SEM results confirmed that the three-dimensional crystal growth was the dominating mechanism of the one-step crystallization process of the parent glass.

To evaluate the comprehensive properties of the glass-ceramics prepared by the one-step crystallization, some properties are shown in Fig. 7. The microhardness and density of the glass-ceramics increased first and then decreased with the heat treatment temperature, as shown in Fig. 7. The increase in density and microhardness may be due to the formation of more augite crystals. Nevertheless, the reason for the decrease in density and microhardness may be that the distance between the augite crystal faces increased with the heat treatment temperature, as discussed above. Other properties of the sample heat treated at 780 ℃ for 1 h are also shown in Fig. 7, and are superior to the similar glass-ceramics prepared by the two-stage heat treatment and sintering methods[3]. The excellent properties of the glass-ceramics suggest its potential applications in construction and industrial areas[19]. In general, all of the above results clearly confirm that the one-step heat treatment is applicable for the glass-ceramics production.

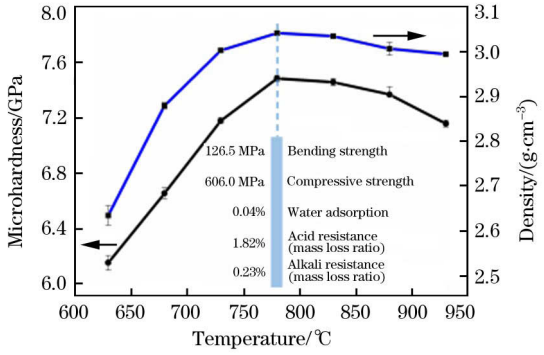

Fig. 7 Properties of the obtained glass-ceramics

3 Conclusion

There have been no crystallization kinetics studies focused on the one-step crystallization of glass-ceramics due to few glass-ceramics prepared by this route. This paper focused on this problem. The activation energy value and the Avrami parameter of the parent glass were calculated as 152.79 kJ/mol and 4.39, respectively. Continuous nucleation and three-dimensional crystal growth were the dominating mechanisms in the one-step crystallization process of the parent glass. The properties of the obtained glass-ceramics were superior to the glass-ceramics prepared by the two-stage heat treatment and sintering method.

References:

[1] N. Karpukhina, R. G. Hill, R. V. Law, Che. Soc. Rev. 43 (2014) 2174-2186.
[2] C. S. Fan, K. C. Li, Ceram. Int. 40 (2014) 7117-7123.
[3] Y. Zhao, D. Chen, Y. Bi, M. Long, Ceram. Int. 38 (2012) 2495-2500.
[4] W. Zhang, H. Liu, Ceram. Int. 39 (2013) 1943-1949.
[5] V. M. F. Marques, D. U. Tulyaganov, S. Agathopoulos, J. M. F. Ferreira, Ceram. Int. 34 (2008) 1145-1152.
[6] R. D. Rawlings, J. P. Wu, A. R. Boccaccini, J. Mater. Sci. 41 (2006) 733-761.
[7] R. D. Rawlings, Glass-ceramic Materials. Fundamentals and Applications, Mucchi Editore, Modena, Italy, 1997.
[8] J. Wu, Z. Li, Y. Huang, F. Li, Ceram. Int. 39 (2013) 7743-7750.
[9] O. A. Lafi, J. Alloys Comp. 519 (2012) 123-128.
[10] X. Guo, X. Cai, J. Song, G. Yang, H. Yang, J. Non-cryst. Solids 405 (2014) 63-67.
[11] L. Lilensten, Q. Fu, B. R. Wheaton, A. J. Credle, R. L. Stewart, J. T. Kohli, Ceram. Int. 40 (2014) 11657-11661.
[12] J. Malek, Thermochim. Acta 267 (1995) 61-73.
[13] M. Abu El-Oyoun, Mater. Chem. Phys. 131 (2011) 495-506.
[14] J. Vázquez, J. L. Cárdenas-Leal, D. García-G. Barreda, R. González-Palma, P. L. López-Alemany, P. Villares, Physica B 405 (2010) 4462-4469.
[15] J. L. Cárdenas-Leal, J. Vázquez, P. L. López-Alemany, P. Villares, R. Jiménez-Garay, J. Alloys Comp. 471 (2009) 44-51.
[16] A. Arslan, H. Koralay, S. Çavdar, A. Günen, J. Non-cryst. Solids 358 (2012) 1190-1195.
[17] E. S. Yousef, H. H. Hegazy, S. Almojadah, Solid State Sci. 23 (2013) 42-49.
[18] J. C. Qiao, J. M. Pelletier, J. Non-cryst. Solids 357 (2011) 2590-2594.
[19] J. Yang, S. G. Zhang, B. Liu, D. A. Pan, C. L. Wu, A. A. Volinsky, J. Iron Steel Res. Int. 22 (2015) 1113-1117.